always enhances T_c substantially as compared to two isotropic order parameters since here low energy scales appear from the *d*-wave channel. The interband coupling also enhances T_c substantially and even at moderate coupling T_c values > 100 K are obtained. A polaronic distortion favors superconductivity as long as the corresponding electron-phonon interaction is not too large. For intermediate to large values of the coupling, superconductivity is rapidly depressed and even vanishes for too strong couplings.

Lattice expansion does not explain the T_c increase in chloroform- and bromoform- intercalated C_{60}

R.E. Dinnebier, O. Gunnarsson, H. Brumm, E. Koch, and M. Jansen;
P.W. Stephens and A. Huq (SUNY Stony Brook)

The groundbreaking experiments of J.H. Schön *et al.* have demonstrated that chemical doping is not the only way to make the fullerenes metallic and superconducting. Using a field-effect transistor setup they showed that pristine C_{60} can be field-doped and becomes superconducting with transition temperatures T_c up to 11 K for electron doping [J.H. Schön *et al.*, Science **288**, 656 (2000)] and 52 K for hole-doping [J.H. Schön *et al.*, Nature **408**, 549 (2000)]. For the chemically electron doped fullerenes it is known that T_c increases with the lattice constant, which is explained by the corresponding increase in the density of states [O. Gunnarsson, Review of Modern Physics **69**, 575 (1997)]. This was the motivation for investigating fullerene crystals intercalated with inert molecules that act as spacers to expand the lattice. And, indeed, it was found that T_c increases to spectacularly high values of 80 K for $C_{60}{\cdot}2CHCl_3$ and 117 K for $C_{60}{\cdot}2CHBr_3$, seemingly confirming the assumption that in order to increase T_c one simply has to increase the density of states [J.H. Schön *et al.*, Science **293**, 2432 (2001)].

Here we report structural determinations of the $C_{60}{\cdot}2CHCl_3$ and $C_{60}{\cdot}2CHBr_3$ co-crystals and give a comparison with pristine C_{60}. We find that intercalation of chloroform and bromoform indeed increases the volume per C_{60} molecule. That increase is mainly due to an expansion of the lattice perpendicular to the closest-packed planes, which are presumably the free surface on which the superconducting FET's have been grown; the area per fullerene remains essentially uncharged. In contrast to chemically electron-doped fullerenes, which are bulk superconductors, superconductivity in the field doped materials is confined to the immediate neighborhood of the surface. The prepared surface is not necessarily a simple truncation of bulk; for example there may be reconstruction, different fullerene orientations, a different concentration of intercalants, etc. However, it is reasonable to expect that the lattice spacings of the 3D structure should persist to the surface, and therefore estimates of the density of states (DOS) derived from the 3D structure will provide a useful insight into the superconductivity. To understand the effect of intercalation on the DOS at the Fermi energy, we have performed tight-binding calculations. We find that, in contrast to what one would expect based on the increase in T_c, the DOS for pristine C_{60} is actually larger than for the co-crystals. Comparing $C_{60}{\cdot}2CHCl_3$ and $C_{60}{\cdot}2CHBr_3$ we find that although the DOS differs slightly, this is by far not enough to explain the difference in the observed transition temperatures.

$C_{60}{\cdot}2CHBr_3$ and $C_{60}{\cdot}2CHCl_3$ were obtained by dissolving C_{60} in bromoform/chloroform with further evaporation. High resolution X-ray powder diffraction data of $C_{60}{\cdot}2CHCl_3$ and

C_{60}·2CHBr$_3$ were collected at various temperatures in a closed cycle helium cryostat at a wavelength of 1.15 Å on beamline X3B1 of the Brookhaven National Synchrotron Light Source in transmission geometry with the samples sealed in 0.7 mm lithiumborate glass capillaries (Fig. 65).

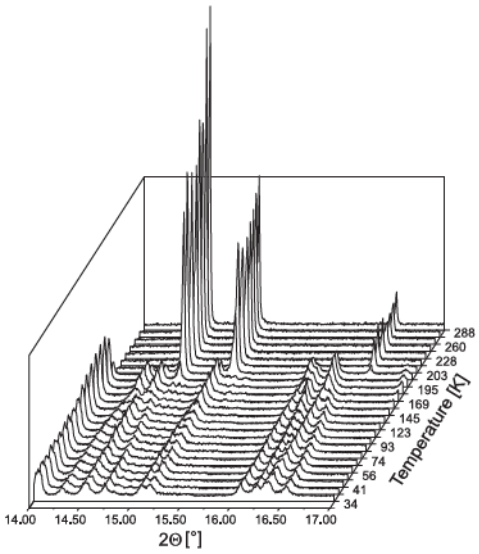

Figure 65: *Scattered X-ray ($\lambda = 1.15015(2)$ Å) intensity for C_{60}·2CHCl$_3$ as a function of diffraction angle 2Θ and temperature T. The temperature range of each scan is on the order of 10 K (cooling on the fly).*

The crystal structure of the different phases of C_{60}·2CHBr$_3$ and C_{60}·2CHCl$_3$ were determined by Rietveld refinements using flexible rigid bodies (Fig. 66). At room temperature, C_{60}·2CHCl$_3$ and C_{60}·2CHBr$_3$ are isotypic to magnesiumdiboride (space group P6/mmm, aluminumdiboride structure type) in which a primitive hexagonal packing is formed by C_{60} molecules with the trigonal prismatic voids at (1/3, 2/3, 1/2) and (2/3, 1/3, 1/2) fully occupied by chloroform or bromoform molecules, respectively. Therefore the structure can be viewed as a sequence of alternating layers of C_{60} and intercalated molecules perpendicular to the *c*-axis. With a six-fold axis through the center of the bucky ball (molecular symmetry $3\overline{m}$) and inversion centers in the center of the chloroform and bromoform molecules (molecular symmetry 3*m*), a minimum of twofold disorder is created, whereas Rietveld refinements confirm almost spherical shell electron density for the C_{60} molecule and at least threefold disorder for the chloroform molecules [G. Waidmann *et al.*, Zeitschrift für Anorganische und Allgemeine Chemie **621**, 14 (1995)].

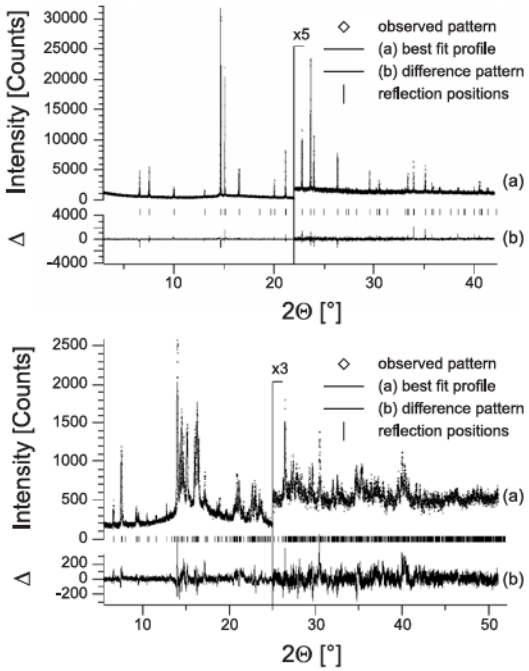

Figure 66: *The scattered X-ray intensity for C_{60}·2CHCl$_3$ at T = 295 K (top), and T = 50 K (bottom) as a function of diffraction angle 2Θ. Shown are the observed patterns (diamonds), the best Rietveld-fit profiles (line) and the difference curves between observed and calculated profiles in an additional window below. The high angle parts of the room temperature and the low temperature phase are enlarged for clarity.*

Upon cooling, both materials pass through a monoclinic phase (which will be discuss elsewhere) into a fully-ordered low temperature triclinic phase (space group $P\overline{1}$) at $\approx$ 150 K with cell dimensions similar to those of the hexagonal room temperature phase. The crystal structure of the triclinic low temperature phase may be viewed as an anisotropically distorted hexagonal room temperature structure. Whereas the

dimensions of the hexagonal closed packed layers of C_{60} molecules show only small distortions when compared to the room temperature structure, the distance between the C_{60} layers (triclinic *b*-axis) increases considerably, causing a decrease in dimensionality. The C_{60} molecules are oriented such that two hexagons on opposite side of the C_{60} molecule are congruent with the triclinic *b*-axis (corresponding to the hexagonal *c*-axis) running through the centers of the hexagons and one of their three short carbon-carbon bonds oriented parallel to *c*-axis (Fig. 67). This way, eight short bonds of a C_{60} molecule (two in *pm a*- and *pm c*-direction each) face short bonds of neighbor molecules with twisting angles between 60 and 90°.

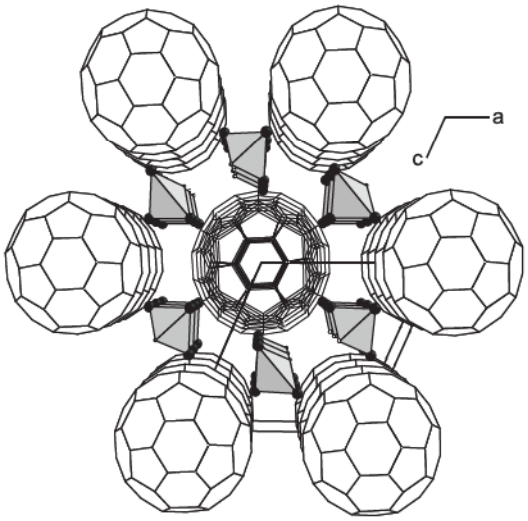

Figure 67: *Crystal structure of the low temperature phase of C_{60}·2CHCl$_3$ at T = 50 K (isotypic to C_{60}·2CHBr$_3$) in a view along b-axis showing the close relationship to the hexagonal room temperature phase.*

The differences in the orientation of the C_{60} molecules between the low temperature phases of C_{60}·2CHCl$_3$ and C_{60}·2CHBr$_3$ are only marginal. The shortest carbon-carbon distances occur between the C_{60} molecules within a layer along the *a*- and *c*-axis (≈ 3.3 Å). In contrast, the shortest carbon-carbon distances between C_{60} molecules of consecutive layers is increasing considerably when going from chloroform (≈ 3.6 Å) to bromoform (≈ 3.8 Å) doped C_{60}, which is in accordance with the observed increase in the lattice parameters.

The orientation of the chloroform and bromoform molecules in the two trigonal prismatic voids are related by inversion symmetry. Two halogene atoms point towards the middle between two C_{60} molecules of consecutive layers, whereas the third halogen atom points either up or down. Consecutive voids along the *b*-axis show the same orientation. The decrease of disorder from the hexagonal to the triclinic structures is accompanied by a loss of long range order and a decrease of the average coherence length (domain size) from approximately 7 μm down to 0.2 μm (in case of C_{60}·2CHCl$_3$) causing severe peak broadening. It should be noted that despite the low quality of the powder patterns at low temperature, the weighted profile R-value (R-wp) of the triclinic low temperature phase is sensitive enough to determine the orientation of the C_{60} molecule within reasonable accuracy: The R-wp of a completely misaligned C_{60} molecule deviates by more than 3%.

Heating-cooling cycles showed pronounced hysteresis (up to 40 K) and coexistence of the different phases over a large temperature range. In general, the transition temperature and the existence of the different phases of C_{60}·2CHCl$_3$ and C_{60}·2CHBr$_3$ depends strongly on their thermal history. In the case of C_{60}·2CHCl$_3$, additional intermediate phases of low symmetry occurred during slow cooling. At the low temperatures where superconductivity is observed basically all material is transformed into the thermodynamically stable low temperature phase as described above.

To describe the electronic structure of C_{60}·2CHCl$_3$ and C_{60}·2CHBr$_3$ we have set up a tight-binding formalism that properly describes the variation of T_c for A_3C_{60} (A = K, Rb). We put one radial 2*p* orbital on each carbon atom and calculate the molecular orbitals (MO) of a

free C_{60} molecule. Only the five-fold degenerate h_u MO is kept, and the hopping integrals between the h_u MOs on different molecules are calculated. The resulting Hamiltonian matrix is diagonalized. The $CHCl_3$ and $CHBr_3$ molecules are neglected in the calculation. Density functional calculations put the highest occupied and lowest unoccupied MOs of a free $CHCl_3$ molecule 1.7 eV below and 2.5 eV above the h_u-orbital of the free C_{60} molecule. These large energetic separations suggest that the $CHCl_3$ molecules contribute little to the structure of the h_u-derived band. The same should be true for $CHBr_3$. We consider the close-packed (010) surface of triclinic $C_{60}{\cdot}2CHCl_3$ (resp. Br) and the (111) surface of cubic pristine C_{60} in the $Pa\bar{3}$ space group. Since, due to the strong electric field, only the surface layer is believed to be doped, we study the corresponding two-dimensional lattices of C_{60} molecules arranged in an (approximately) hexagonal structure. This approach neglects the effects of the strong electric field on the surface layer and the (weak) coupling to the underlying layers.

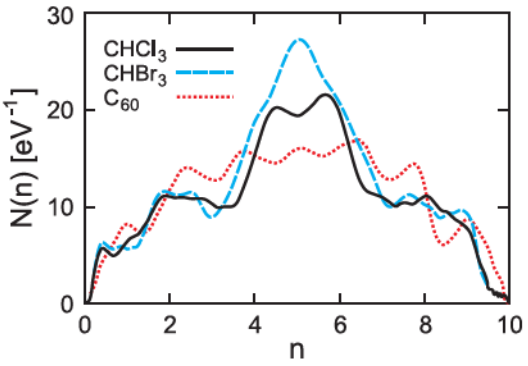

Figure 68: *Density of states N(n) at the Fermi energy as a function of the doping n. The figure compares results for the (010) surface of $C_{60}{\cdot}2CHCl_3$ and $C_{60}{\cdot}2CHBr_3$ and the (111) surface of pure C_{60}.*

Figure 68 shows the calculated density of states (DOS). The largest difference to the bulk is the reduced number of neighbors at the surface from eight to six for the $P\bar{1}$ (010) surface and from twelve to six for the $Pa\bar{3}$ (111) surface. This results in a reduced band width and an increased DOS. The DOS for C_{60} and $C_{60}{\cdot}2CHCl_3$ in Fig. 68 are comparable, but the DOS of C_{60} is larger for doping from about 2 to 3.5 where substantial T_c's have been observed. Based on the DOS one would thus expect T_c for C_{60} to exceed that of $C_{60}{\cdot}2CHCl_3$ – in contrast to experiment.

The orientations of the C_{60} molecules in the different structures play, however, an important role. Actually the surface area per molecule for $C_{60}{\cdot}2CHCl_3$ (86.5 Å^2) is slightly larger than for C_{60} (85.4 Å^2). The hopping between the molecules is, nevertheless, somewhat stronger for $C_{60}{\cdot}2CHCl_3$. The reason is that it mainly takes place via a few 'contact atoms'. The hopping is thus very sensitive to the relative phases of the h_u-orbitals at these atoms. These phases are relatively unfavorable for the $Pa\bar{3}$ structure of pure C_{60}, making the hopping somewhat weaker. To illustrate this, we rotated the C_{60} molecule in $C_{60}{\cdot}2CHCl_3$ by just 5° around the *b*-axis. This increases the second moment $\langle\varepsilon^2\rangle$ of the DOS by 15%. Rotating the molecules around the three crystallographic axes we find that $\langle\varepsilon^2\rangle$ changes by factors in the range 0.75–2.36. Since the DOS behaves roughly as $1/\sqrt{\langle\varepsilon^2\rangle}$, this suggests that a change in the C_{60} orientation is likely to decrease the DOS and a possible increase should be at most 15% for $C_{60}{\cdot}2CHCl_3$, still leaving it smaller than for C_{60}.

Comparing $C_{60}{\cdot}2CHCl_3$ and $C_{60}{\cdot}2CHBr_3$ is even more clear-cut since they basically only differ by their lattice constants, while the relative orientations of the molecules are similar. In the doping range 2 to 3.5 the DOS is increased by at most 10%. Solving the isotropic Eliashberg equations using realistic parameters we find, however, that the DOS of $C_{60}{\cdot}2CHBr_3$ would have to be about 25 to 35% larger than for $C_{60}{\cdot}2CHCl_3$ in order to explain the change in T_c. Thus even for the structurally similar intercalated crystals the increase in T_c cannot be understood as a result of the expansion of the lattice alone.

What might then be the reasons for the observed strong enhancement of T_c? What comes to mind first is that superconductivity may not be limited to the surface layer. However, to obtain a substantial doping, the levels in the surface layer have to be well separated from those in the layers underneath. Therefore their contribution to the DOS can be expected to be small. Also the strong electric field in the surface layer may play an important role. A simple estimate suggests, however, that its effect on the DOS should not be very large. There also could be some coupling to the vibrational modes of the $CHCl_3$ and $CHBr_3$ molecules, which might tend to enhance T_c. The large separation of their levels from the C_{60} h_u-orbital suggests, however, that this coupling is weak. Finally, as discussed above, the DOS can be quite sensitive to the orientations of the C_{60} molecules. It is conceivable that they could be different at the surface. For instance, the $CHCl_3$ and $CHBr_3$ molecules, having a dipole moment, would tend to align with the electric field at the surface, possibly influencing the orientations of the C_{60} molecules. The surface of pristine C_{60} could also be reconstructed in such a way that its DOS is reduced.

Above we have based our discussion on the DOS at the Fermi energy, as has been done in the past. This describes the variation of T_c for A_3C_{60} well, i.e., as a function of the lattice parameter for fixed doping. However, it does not describe the strong doping dependence of T_c, since the DOS of the merohedrally disordered A_3C_{60} is rather constant. In addition, for the electron-doped systems, field-doping and chemical doping give similar values of T_c. This is surprising, since the reduced number of neighbors at the surface should lead to a larger DOS and a correspondingly higher T_c. These problems raise questions about the conventional interpretation just in terms of the density of states.

Magnetic resonant mode in a single-layer high temperature superconductor

H. He, C. Ulrich, and B. Keimer; Y. Sidis, P. Bourges, and L.P. Regnault (CEA, France);
N.S. Berzigiarova and N.N. Kolesnikov (Russian Academy of Sciences)

Electronic conduction in the copper oxide high temperature superconductors takes place predominantly in structural units of chemical composition CuO_2, in which copper and oxygen atoms form an approximately square planar arrangement. Most theoretical models of high temperature superconductivity are therefore based on a two-dimensional square lattice. In real materials, however, deviations from this simple situation are nearly always present. For instance, buckling distortions of the CuO_2 layers that are found in many copper oxides are thought to have a significant influence on the electronic structure and on the superconducting transition temperature T_c. Interlayer interactions in materials with closely spaced CuO_2 layers (forming bi- or trilayer units) or additional copper oxide chains in the crystal structure present further complications whose influence on the superconducting properties remains a subject of debate. Experiments on $Tl_2Ba_2CuO_{6+\delta}$, a material with unbuckled, widely spaced CuO_2 layers and a maximum T_c around 90 K, have therefore played a pivotal role in resolving some issues central to our understanding of these materials.

We have performed inelastic neutron scattering measurements of $Tl_2Ba_2CuO_{6+\delta}$ near optimum doping ($T_c \approx 90$ K) that provide evidence of a sharp magnetic resonant mode below T_c. A resonant spin excitation of this kind has been ex-